Chapter 7

Preparation and characterization of diverse dipyridamole formulations

7.1 Dipyridamole-Drug Profile

Dipyridamole (DPL) is a platelet inhibitor used in treatment of variety of heart disease [1-3].

General Characteristics: [4-8]

- **Molecular Formula:** $C_{24}H_{40}N_8O_4$
- **IUPAC Name:** 2,2',2",2'"-[(4,8-Dipiperidinopyrimido [5,4-d] pyrimidine -2,6 -diyl) dinitrilo] tetraethanol
- **Structure:**

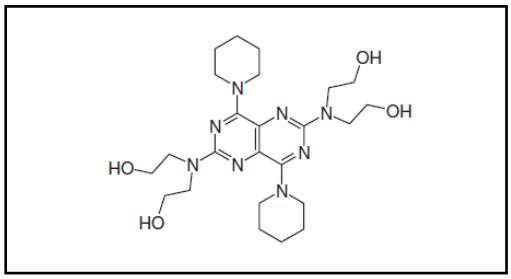

- **Molecular weight:** 504.625
- **Appearance and Color:** Yellow crystalline powder.
- **Odor:** Odorless.
- **Solubility:** Soluble in dilute acids having pH 3.3 or below, methanol, ethanol, chloroform and slightly soluble in water.
- **Melting point:** 162 to 168^{o}C.
- **Dissociation constants:** pKa of 6.4.
- **Octanol/Water Partition Coefficient**: log P = 1.5.
- **Dose**: 25 mg, 50 mg and 75 mg.

Mechanism of action

Dipyridamole inhibits platelet aggregation by various mechanisms. It inhibits phosphodiesterase enzyme in platelets thereby restricting the breakdown of cAMP level and increasing the cellular concentration of cAMP in platelets. Secondly it inhibits the uptake of adenosine in platelets, endothelial cells and erythrocytes which increases the concentration of adenosine at the platelet vascular interface. The adenosine stimulates the platelet adenylate cyclase and increases the platelets cAMP levels. The third mechanism states potentiation of prostaglandin I2 (PGI2) antiaggregatory activity and enhancement of PGI2 biosynthesis. Thus, all these

independent processes inhibit the platelet function by increasing the cAMP level or through stimulation of cAMP formation [6, 8-10].

Pharmacokinetics

The absolute bioavailability of dipyridamole is reported in range of 18-44%. The time to reach peak plasma concentration is about 75 minutes after oral administration. It is highly bound to plasma proteins. It is metabolized in the liver and excreted mainly as glucoronide conjugate in the bile. A little amount is excreted in urine. [2, 6, 8].

Indications and Usage

For treatment and prevention of postoperative thromboembolic complications and cerebrovascular diseases. Moreover it is also been widely used to inhibit and cure angina, prevent recurring myocardial infarction and thrombosis in clinical situations [1-3].

Contraindications

Dipyridamole is contraindicated in known cases of hypersensitivity to the drug [8].

Drug Interactions

Dipyridamole increases the cardiovascular effects and plasma levels of adenosine. It may counteract the anticholinesterase effect of cholinesterase inhibitor [8].

Adverse Effects

Adverse effects observed with dipyridamole are generally transient and minimal. Some of them reported from uncontrolled studies include diarrhea, vomiting, pruritus and flushing. Liver dysfunction has been rarely reported [8].

7.2 Analytical methods

7.2.1. Determination of DPL in phosphate buffer pH 6.8 at 412 nm by UV – spectrophotometric method

Method was used for estimation of DPL in solubility studies and dissolution in pH 6.8 phosphate buffer for the preliminary trial batches.

7.2.1.1. Preparation of standard stock solutions of DPL

DPL (100 mg) was dissolved in 50 ml of methanol: phosphate buffer pH 6.8 and volume was made up to 100 ml with phosphate buffer pH 6.8 to obtain stock solution of 1000 µg/ml. An aliquot of 10 ml was accurately taken out with graduated calibrated pipette and further diluted upto 100 ml with phosphate buffer pH 6.8 to obtain working standard solution of 100 µg/ml.

7.2.1.2. Preparation of calibration curve of DPL

Varying concentrations of DPL (10-60 µg/ml) were prepared with appropriate dilutions of stock solution with phosphate buffer pH 6.8. using UV spectrophotometer (Shimadzu UV 1700, Japan) with 1 cm quartz cuvettes and calibration curve was plotted against concentration (µg/ml).

Accuracy and precision were carried out as per ICH guidelines [11]. For accuracy measurements were taken in triplicate and for precision six determinants were measured. The results of accuracy and precision are depicted in Table 1 and Table 2 respectively. No interference of excipients was found at specified detection wavelength. The reference spectrum of DPL is depicted in Fig. 1. The calibration curve of DPL in phosphate buffer pH 6.8, regression analysis equation and correlation coefficient is depicted in Fig. 2.

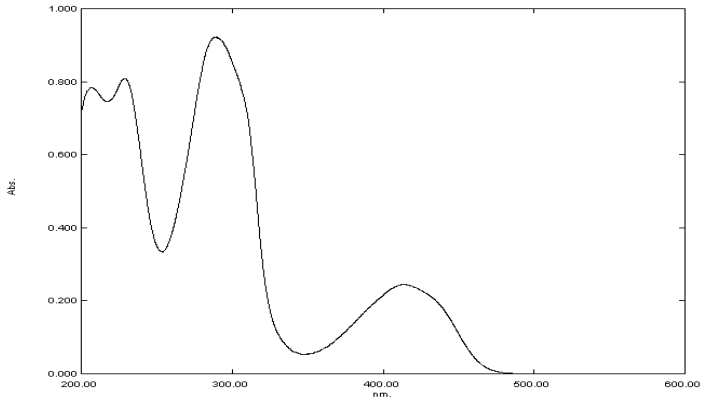

Fig. 1: Reference spectra of DPL in phosphate buffer pH 6.8 at 412 nm.

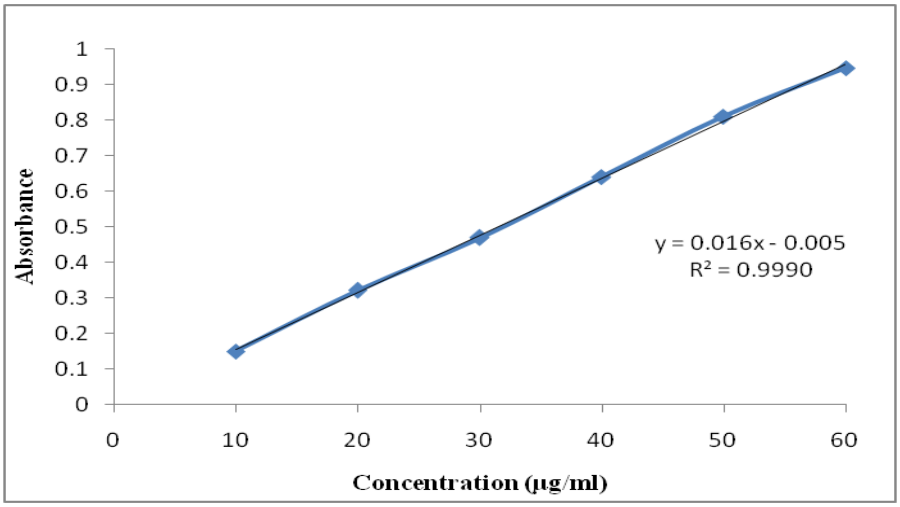

Fig. 2: Calibration curve of DPL in phosphate buffer pH 6.8 at 412 nm.

% Recovery:

Table 1: % Recovery for DPL

Amount of Sample Taken Equivalent to (mg)	Amount of Sample Spiked (mg)	Amount of Spiked Sample Recovered	% Recovery
20	12	12.10±0.10	100.83
20	20	20.09±0.18	100.45
20	28	27.89±0.15	99.61

Data are represented as Mean± SD (n=3)

Precision:

Table 2: Precision for DPL

	% Relative Standard Deviation
Repeatability	0.82
Intraday	1.28
Interday	1.62

7.2.2. Determination of DPL by reverse phase high performance liquid chromatography method RP-HPLC:

Method was used for estimation of DPL during dissolution in 0.1N HCL, pH 6.8 phosphate buffer, solubility studies and drug content in formulation and final optimization batches.

7.2.2.1. HPLC instrumentation and conditions

Chromatography was performed on Shimadzu (Shimadzu Corporation, Kyoto, Japan) chromatographic system equipped with Shimadzu LC-20AT pump and Shimadzu SPD-20AV UV detector. Samples were injected through a Rheodyne 7725 injector valve with fixed loop at 20 µL. The chromatographic separation was performed using a Shodex C18 (250 mm × 4.6 mm i.d., 5 µm particle size) column. The mobile phase was vacuum filtered through 0.22 µm nylon membrane filter followed by degassing in an ultrasonic bath prior to use. Data acquisition and integration was performed using Spinchrome software (Spincho Biotech, Vadodara). Table 3 represents HPLC parameters for determination of DPL.

Table 3: HPLC parameters for estimation of DPL.

Parameter	Condition
Column	Shodex C18 (250 mm × 4.6 mm i.d., 5 µm particle size)
Mobile Phase	Methanol:Water:TEA (70:30:0.1); pH 3.5 adjusted with orthophosphoric acid.
Flow rate	1 ml/min
Detection wavelength	238 nm
Injection volume	20 µl

7.2.2.2. Preparation of standard stock solution of DPL

DPL (100 mg) was dissolved in 30 ml of mobile phase and volume was made up to 100 ml with mobile phase in to obtain stock solution of 1000µg/ml. An aliquot of 10 ml was accurately taken out with graduated calibrated pipette and further diluted upto 100 ml with mobile phase to obtain working standard solution of 100 µg/ml.

7.2.2.3. Preparation of calibration curve of DPL

Varying concentrations of DPL (10-100 µg/ml) were prepared with appropriate dilutions of stock solution with mobile phase. Calibration graph was constructed by plotting area versus concentration of DPL and the regression equation was calculated. The calibration curve of DPL, regression analysis equation and correlation coefficient is depicted in Fig. 3 and reference chromatogram is depicted in Fig. 4. System suitability test was performed by injecting six consecutive samples of 30µg/ml during start of method validation. The parameters observed were retention time, tailing factor, theoretical plates and %relative standard deviation (%RSD) of area. The data are represented in Table 4. The accuracy and precision data are represented in Table 5 and Table 6 respectively.

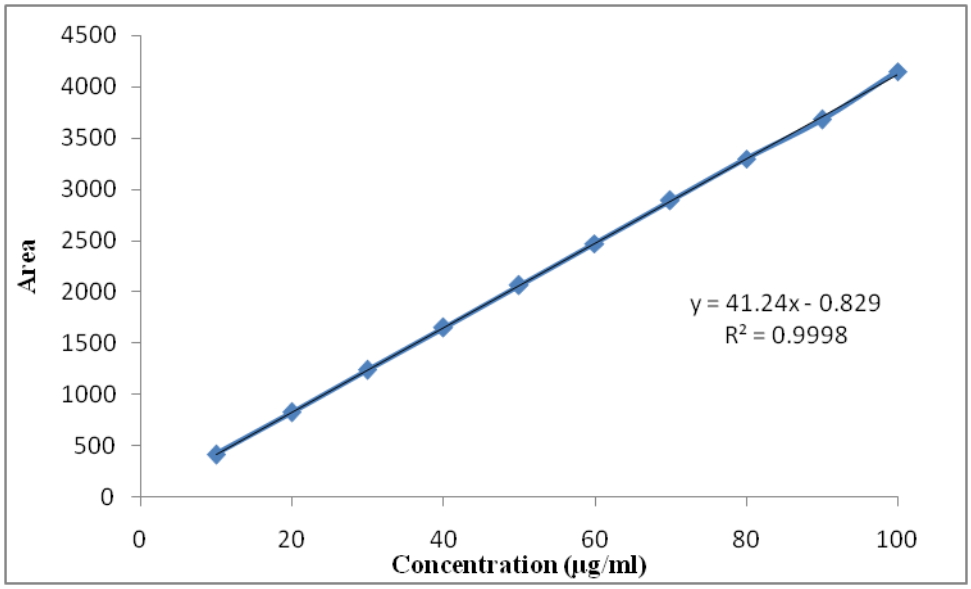

Fig. 3: Calibration curve of DPL taken using HPLC method.

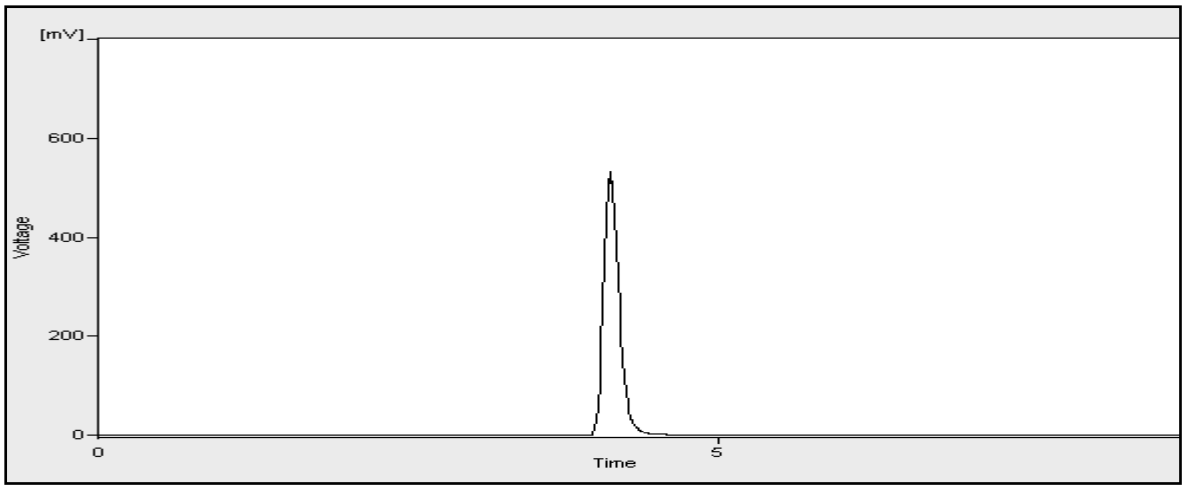

Fig 4: Reference chromatogram of DPL obtained by performed HPLC method.

System suitability parameters

Table 4: System suitability parameters for estimation of DPL

Parameters	Mean±SD
Retention time (min)	4.8±0.08
Asymmetry	1.12±0.06
Theoretical plate	8885.5±53.55
%RSD of area	1.38

% Recovery:

Table 5: % Recovery for DPL

Amount of Sample Taken Equivalent to (mg)	Amount of Sample Spiked (mg)	Amount of Spiked Sample Recovered	% Recovery
20	12	11.89±0.06	99.08
20	20	20.12±0.18	100.6
20	28	27.95±0.09	99.82

Data are represented as Mean± SD (n=3)

Precision:

Table 6: Precision for DPL

	% Relative Standard Deviation
Repeatability	1.29
Intraday	1.51
Interday	1.90

7.3. Methods

7.3.1. Preparation of DPL – additives binary systems

DPL-HPMC and DPL-PVP binary systems and their respective molecular weight grades binary systems were prepared by quench cooling method. Preparation of physical mixtures (PM) of DPL and polymers were carried out using geometric mixing, by triturating in the mortar and pestle. The finely powdered mixture was taken in stainless steel beaker and heated upto around 168 ^{o}C followed subsequently by quench cooling of the melt over crushed ice. The quench cooled product was grounded and sifted through ASTM#45 for further usage. The purity of the quench cooled product was assessed by HPLC method. The HPLC analysis revealed 99.99% purity of sample confirming no degradation occurred during the preparation of amorphous system.

The polymers having different physical and chemical attributes were selected to study their effects on stabilization of DPL supersaturation upon transition from acidic pH of stomach to around neutral pH of intestine. Reports have been found in the literature suggest role of molecular interactions in solutions, steric hindrance or combination of both as mechanisms for improving supersaturation by polymeric carriers in the solutions [12-16]. Thus, here HPMC and PVP which have contrasting hydrogen bond characteristics viz., PVP which is proton acceptor and HPMC which is proton donor were selected for evaluating intermolecular interactions and their respective different molecular weight grades for evaluating steric hindrance mechanism of stabilization. For HPMC, three viscosity grades were investigated viz; HPMC E5, HPMC E15 and HPMC E50 and for PVP two grades were investigated PVP K30 and PVP K90.

DPL-fumaric acid binary systems were also prepared in the similar manner as discussed above.

7.3.2. Solubility studies

The dynamic or equilibrium aqueous solubility of crystalline, amorphous, various PMs, solid dispersions (SDs) of DPL and complex of DPL with fumaric acid was determined by adding excess solid (150 mg) to 25 ml of precipitating medium phosphate buffer pH 6.8 in stoppered conical flasks which was pre-equilibrated at 37 ± 0.5°C. The flasks were placed on magnetic stirrer with heater (Remi Sales & Engineering Ltd., India) at 300 rpm. At predetermined time intervals samples were withdrawn, filtered through a 0.45 µm filter and analyzed using UV-spectrophotometric and HPLC method as discussed in section 7.2. Solubility studies of the PMs of the drug and excipient (50% w/w) for PVP K-90 and HPMC E50 and 30%w/w for fumaric acid were also performed in phosphate buffer pH 6.8. All measurements were made in triplicate. The statistically significant differences were investigated using one way ANOVA (Graphpad Prism 5.0, USA) between various parameters at 5% significance level ($p<0.05$). Post-hoc analysis was carried out using Dunnett's Multiple Comparison Test and Bonferroni's Multiple Comparison Test.

7.3.3. *In vitro* dissolution studies

Dissolution experiments of crystalline DPL, PM with HPMC E50, PVP K90 and fumaric acid and SDs/complex samples were carried out to evaluate *in vitro* drug release profile. Dissolution studies were performed using United States Pharmacopeia (USP) 30 type II apparatus (VDA 6-DR, Veego Instruments Corporation, Mumbai, India) using 900 ml of precipitating medium pH 6.8 phosphate buffer at 50 rpm rotation speed and 37 ◦C±0.5 ◦C temperature. Samples of crystalline DPL, PM and SDs/complex equivalent to 50 mg of the drug was added to the dissolution medium. An equal volume of pre-warmed fresh medium at same temperature was replaced in the vessel after each sampling to maintain constant volume throughout the test. Dissolution profiling and data were recorded at 5, 15, 30, 45, and 60 min. Samples withdrawn were filtered through a 0.45 µm membrane filter, appropriately diluted and then analyzed for drug release by analytical methods as discussed in section 7.2. Preliminary tests revealed that the method was specific for estimation of DPL and no interference was observed due to additives dissolved in the dissolution medium. Finally, cumulative % of drug released was calculated and plotted against function of time to study the pattern of drug release.

7.3.4. Supersaturated dissolution testing

To assess the ability of the SDs with PVP/HPMC and complex with fumaric acid for maintaining supersaturation of DPL following an acidic to neutral pH change, *in vitro* dissolution studies was carried out in pH change over media according to the method A for delayed release dosage form mentioned in USP [17]. Here, for first 2 h dissolution was carried out in 750 ml of 0.1 N hydrochloric acid (HCL) followed by addition of 250 ml of 0.2 M tribasic sodium phosphate adjusted to pH 6.8 for additional 4 h using USP apparatus-II, 50 rpm rotation speed and 37 ◦C±0.5 ◦C temperature.

7.3.5. Formulation studies

Preliminary screening was carried out for selection of excipients based on their compatibility with drug and analytical method specificity for DPL. Rapidly disintegrating tablets containing equivalent 50 mg of DPL were prepared by direct compression method using diverse formulation excipients like directly compressible lactose, microcrystalline cellulose, sodium starch glycolate, colloidal silicon dioxide and magnesium stearate. The blend was compressed on an eight station automatic rotary tablet machine (JM-8, General Machinery Co., Mumbai, India) equipped with standard concave punches of 10.0 mm diameter to obtain target tablet weight of 400 mg. The release profile of drug from tablets was studied from six dosage units using the same dissolution media, conditions, and procedure as described for *in vitro* dissolution studies.

7.3.6. Statistical analysis

7.3.6.1. Similarity factor f2

A model independent approach was employed for comparing dissolution profiles of variegated samples by calculating similarity factor f2 [18]. The similarity factor f2 is a measure of similarity in the percentage dissolution between two dissolution curves and is defined by following eq. 1:

$$f_2 = 50\log\left\{\left(1 \div \frac{1}{\mathrm{n}}\sum_{t=1}^{n}(R_t - T_t)^2\right)^{-0.5} \text{ x } 100\right\} \qquad (1)$$

where n is the number of withdrawal points, R_t is the percentage dissolved of reference at time point t, and T_t is the percentage dissolved of test at time point t. f2

value of 100 indicates reference and test profiles are identical. Values between 50 and 100 signify that the dissolution profiles are similar, while lower f2 values suggests an increase in dissimilarity between release profiles.

7.3.6.2. Similarity factor Sd

The similarity factor Sd is given by below eq. 2

$$Sd = \frac{\sum_{t=1}^{n=1} \left| \text{Log}((AUC_{Rt}) / (AUC_{Tt})) \right|}{n - 1} \quad (2)$$

where *n* is the number of data points collected during the *in vitro* dissolution test; AUC_{Rt} and AUC_{Tt} are the areas under curves of the dissolution profiles of the reference and test formulations, at time t. For the test and reference formulations to be identical, the Sd value should be zero. Sd values increase with increase in percentage difference between dissolution profiles [19, 20].

7.3.6.3. Rescingo index (ξ)

The method was initially developed to compare plasma drug concentrations as function of time. It can also be use to compare dissolution profiles between test and reference formulations. It can be expressed as below eq. 3

$$\xi_i = \left\{ \frac{\int_0^{\infty} |d_R(t) - d_T(t)|^i \, dt}{\int_0^{\infty} |d_R(t) + d_T(t)|^i \, dt} \right\}^{1/i} \quad (3)$$

where $d_R(t)$ is the reference product dissolved amount, $d_T(t)$ is the test product dissolved amount at each sample, time point respectively The value of rescingo indices lye between 0 and 1. The index is 0 when the two dissolution release profiles are identical and 1 when the drug from the reference or test formulation is not released at all [21, 22].

7.3.6.4. Mean dissolution time (MDT)

Mean dissolution time (MDT) reveals the time for the drug to dissolve and is the first statistical moment for the cumulative dissolution process that provides an accurate

drug release rate [23]. To understand the extent of improvement in dissolution rate of DPL from its PMs and SDs with PVP and HPMC, the obtained dissolution data of all samples were fitted into the eq. 4

$$MDT = \frac{\sum_{i=1}^{n} t_{mid} \Delta M}{\sum_{i=1}^{n} \Delta M} \quad (4)$$

where i is the dissolution sample number, n is the number of dissolution times, t_{mid} is time at the midpoint between times t_i and t_{i-1}, and ΔM is the amount of DPL dissolved between times t_i and t_{i-1}.

7.3.6.5. Dissolution efficiency (DE)

The dissolution efficiency (DE) [24, 25] is defined as the area under the dissolution curve up to a certain time, t, expressed as a percentage of the area of the rectangle described by 100% dissolution in the same time. It can be calculated by below following eq. 5.

$$DE = \frac{\int_0^t y \, dt}{y_{100} \times t} \times 100\% \quad (5)$$

where y is the drug percent dissolved at time t.

7.3.7. Characterization of solid dispersion

7.3.7.1. Differential scanning calorimetry (DSC) study

DSC thermograms of pure DPL, PMs, SDs with different HPMC and PVP grades and complex with fumaric acid were obtained using an automatic thermal analyzer system (DSC-60, Shimadzu, Japan). The (3-5 mg) sample was crimped in a standard aluminum pan and heated from 40˚C to 200˚C at a heating rate of 5˚C/min under constant purging of dry nitrogen at 40 ml/min. Temperature calibration was performed using indium as the standard. An empty pan, sealed in the same way as the sample, was used as the reference.

7.3.7.2. Fourier transform infra-red (FT-IR) spectroscopy study

The FT-IR (Bruker, USA) spectra of the pure DPL, PMs, SDs with different HPMC and PVP grades and complex with fumaric acid were investigated using potassium bromide (KBr) pellet method. In brief procedure involved mixing of total of 2% (w/w) of the sample with respect to the KBr (S. D. Fine Chem Ltd., Mumbai, India). The mixture of drug and dry KBr was ground into an agate mortar and was compressed into a KBr pellet under a hydraulic press at10,000 psi. Each KBr disk was scanned 16 times at 4 mm/s at a resolution of 2 cm^{-1} over a wavenumber range of 400–4000 cm^{-1}. The characteristic peaks were recorded.

7.3.7.3.Powder X-Ray Diffraction (PXRD) Study

Powder X-ray diffraction (PXRD) patterns of the pure DPL, PMs, SDs with different HPMC and PVP grades and complex with fumaric acid were investigated employing powder Xray diffractometer (Philips X'Pert, The Netherlands) using CuKa radiation of wavelength 1.54 A˚, a voltage of 40 kV and a current of 40 mA. As the slide moves at an angle of theta degree, a proportional detector detects diffracted X-rays at angle of 2θ° and subsequently XRD patterns were recorded. XRD patterns were recorded in the 2θ° range of 5 to 60.

7.3.8. *In vitro* cell line studies

Cell culture flasks (75 cm^2 with ventilated caps) and Transwell cell culture systems (12 wells, 1.13 cm^2 polyester, 0.4 µm pore size) from Corning (Sigma Aldrich, India) were used. Caco-2 cells, were obtained from National Centre For Cell Science (NCCS Pune, India) at passage 18. Cells were cultured in 75 cm^2 flasks using 25 ml medium and maintained in a humidified, 5 % CO_2, 95 % atmospheric air incubator (ESCO, India) at 37°C. Cell cultured medium was pre-warmed to 37 °C and comprised of 500 ml Dulbecco's modified Eagle medium , 10 % fetal bovine serum, 5 ml nonessential amino acid solution (X100), 5 ml L-glutamine solution (200 mM), and 0.5 ml of gentamycin solution (50 mg/ml). The medium was changed every other day until the flask reached 90 % confluence. Confluent cells were detached using trypsin–EDTA solution. The cell layer was washed twice with 6 ml of pre-warmed (at 37 °C) phosphate buffer saline (PBS). After removal of PBS, 3 ml of trypsin–EDTA was gently dripped down side of the flask to distribute trypsin–EDTA solution all over

surface of the culture. Flask was kept in incubator shaker (Orbitek, Inida) with 30 rpm speed for not more than 2 min to detach the cell. Trypsination was stopped by addition of propagation medium to neutralize trypsin, and then cells were pelleted by centrifugation at 1500 rpm for 5 min. Supernatant was removed and cell pellets were re-suspended in assay medium and counted using a hemocytometer. Cells were seeded onto the Transwells with seeding density 1 X 10^5 cells/cm^2. Cells were introduced to the apical surface of transwell cell culture support in 0.5 ml medium and 1.5 ml medium was added to the basolateral chamber. Cells were incubated at 37 °C with 5 % CO_2 and 90 % relative humidity, and media was changed every 24 hrs for first week and then every 48 hrs. The cells used for transport studies were between 21 and 28 days. The integrity of monolayer was checked by measuring Transepithelial Electrical Resistance (TEER) after each week till transport studies done.

7.3.8.1 Cell monolayer integrity

The initial and final values of TEER of the Caco-2 cell monolayers grown on permeable supports were measured with a ERS voltameter (Millicell® ERS meter). The monolayers were equilibrated for 25-35 min before TEER measurements. Only cell monolayers with TEER values over 200 Ω cm^2 were used. TEER was calculated by subtracting the resistance of a cell-free culture insert and correcting for surface area of the Transwell cell culture support. The TEER value was calculated from the following eq. 6:

$$TEER = (R_{monolayer} - R_{blank}) \times A \quad (6)$$

where R monolayer is the resistance of the monolayer along with filter membrane, R blank is the resistance of the filter membrane and A is the surface area of the membrane (1.13 cm^2 in 12-well plates). The final values of TEER were measured to determine opening of cell tight junctions.

7.3.8.2. Transport Studies

To prepare cell layers on the day of transport studies, TEER was measured and medium on the apical and basolateral chambers was aspirated and cell layers washed twice with pre-warmed (37 °C) Hanks' Balanced Salt solution (HBSS). The cells were allowed to equilibrate in pre-warmed HBSS /HEPES buffer pH 7.4 for half an hour to one hour in the incubator at 37 °C. The TEER was measured prior to experimentation. For absorptive permeability, transport studies was initiated by

adding 0.5 ml of respective test solution to the apical chamber and 1.5 ml to the basolateral chamber. Initially samples were added to pH 6.8 phosphate buffer and mixed it well for 30 minutes by stirring. Then samples were filtered and suitably diluted in HBSS and added to apical chamber. All experiments were performed at 37 °C. Samples (100 µl) were withdrawn from the basolateral chamber at 0, 30, 60, 90, 120, 150, 180 and 240 min and from the apical chamber 20 µl sample withdrawn at 0 and 240 min. The withdrawn volume was replaced with fresh transport media. For all instances, each experiment was performed two times to get n = 6 for control and experimental wells, samples were appropriately measured and averaged. TEER was also measured after final sample withdrawal. The apparent permeability coefficient, P app (cm/s), was calculated from the following eq. 7:

$$P\ app = (dQ/dt)/(C0 .A) \quad (7)$$

where dQ/dt is the cumulative transport rate (µM/min) defined as the slope obtained by linear regression of cumulative transported amount as a function of time (min), A is the surface area of the filters or inserts (1.13 cm^2 in 12-wells) and C0 is the initial concentration of the DPL on the apical side (µM). The drug content was analysed by validated HPLC method as discussed in section 7.2.2.

7.3.8.2. Assessment of cell viability or MTT assay

The excipients and DPL formulations were diluted in water and added to the cell monolayer in 48 well plates and incubated for 4 hr. Placebo formulation represents the formulation without DPL and control samples represents media without excipients. The procedure mentioned in literature was taken as reference for performing MTT assay [26]. Results were recorded using ELISA plate reader (BIO-RAD, India).

7.3.9. Stability studies

The optimized formulation batch prepared for polymer and pH modifier was subjected to short term stability testing according to the ICH guidelines [27]. Tablets were packed in count of 30 into high density polyethylene bottle with child resistant cap and were further induction sealed. Before induction sealed one silica bag was kept in bottle as desiccant. The sealed bottles were exposed to accelerated (40 ± 2^oC/75 ± 5% relative humidity) and long term (25 ± 2^oC/60 ± 5% relative humidity) stability for three months. The samples were withdrawn

periodically (0, 15, 30, 60 and 90 days) and evaluated for different physicochemical parameters like visual inspection, drug content and *in vitro* drug release.

7.4 Results and Discussion

7.4.1. Solubility studies

The solubility studies were carried out in precipitating medium pH 6.8 phosphate buffer. Preliminary trials were investigated with varying ratios of drug:polymer starting from polymer concentration 5%w/w to investigate its effect on solubility and amorphous behavior of SD. From the preliminary trials investigated, 50%w/w ratio of drug: polymer was selected for all polymer types and its molecular weight grades considering factors like solubility, tendency to form amorphous nature and harmonization amongst various grades.

The results of equilibrium solubility of different grades of HPMC and PVP are displayed in Fig. 5. Crystalline DPL, a hydrophobic molecule achieved a maximum equilibrium solubility of 6.53 µg/ml in about 12 h. Additionally, crystalline DPL floated on the medium and sticked to the wall of the flasks. On the other hand glassy DPL sank into the medium but was found to be highly unstable and tend to revert to the crystalline form within 30 min and attained equilibrium solubility similar to that of crystalline form. Thus, the practical advantage of amorphous DPL was totally lost due to its liking to undergo solvent mediated transformation and immediate transition to thermodynamically more stable crystalline form. The culprit in this case was the water which caused plasticization of amorphous system and also the pH of medium where it has more chances of crystallization. The trend was rather different with polymeric excipients. From Fig.5, it can be concluded that the SDs with hydrophilic carriers like HPMC and PVP have proven to stabilize the amorphous form, thus providing enhanced solubility than crystalline form and its PM. The same can be inferred from Table 7 depicting solubility ratio of SDs and PMs with HPMC and PVP. Dunnett's Multiple Comparison Test revealed statistically significant difference ($p<0.05$) between the solubility values of crystalline DPL and that of SDs with PVP and HPMC.

As seen from Fig.5, amongst different molecular weight grades of HPMCs, the highest peak solubility was shown by HPMC E50 followed by HPMC E15 and then by HPMC E5. On the contrary, no significant difference was found in peak solubility values between two molecular weight grades of PVP viz., PVP K30and PVP K 90.

Overall, HPMC was superior in enhancing solubility than PVP which can also be observed from solubility ratio (Table 7).

In case of the pH modifier, preliminary trials were investigated in similar manner as in case of polymeric excipients starting from 5% w/w to investigate its effects on solubility. From the preliminary trials 30%w/w was selected to be optimum as higher concentration did not exhibit significant improvement in solubility. The results of the equilibrium solubility of PM and complex formation is depicted in Fig. 5. From Fig.5, it can be clearly stipulated the influence of complex with pH modifier on increasing the solubility than its PM and crystalline counterparts. The same can be inferred from Table 7 depicting the solubility ratio. Dunnett's Multiple Comparison Test revealed statistically significant difference ($p<0.05$) between the solubility values of crystalline DPL and its complex with fumaric acid.

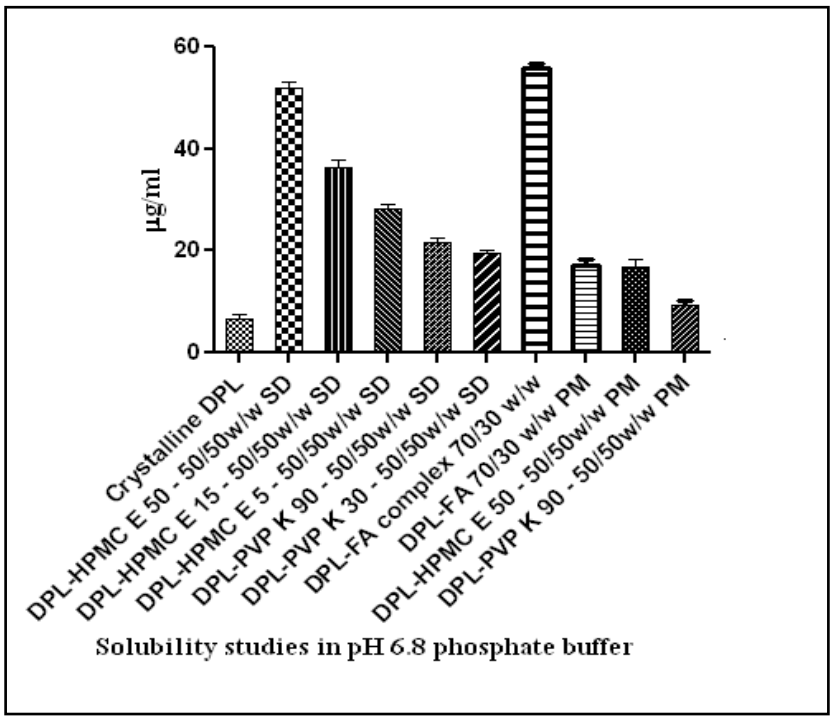

Fig.5: Solubility studies of crystalline dipyridamole, physical mixtures and solid dispersions in pH 6.8 phosphate buffer.

Table 7: **Table representing solubility ratio, various indices for comparison of dissolution profiles, cumulative percent drug released at 30 min (DP_{30min}), Mean Dissolution Time (MDT) and Dissolution Efficiency (DE) for plain drug, physical mixtures, solid dispersions and complex formation.**

	Crystalline DPL	SDHPMC E5	SDHPMC E15	SDHPMC E50	SDPVP K30	SDPVP K90	PMHPMC E50	PMPVP K90	FA# complex	PM FA#
Solubility ratio	-	4.32	5.58	7.96	2.96	3.30	2.56	1.44	8.55	2.65
f2	-	22.99	18.20	8.53	41.27	36.52	49.39	63.55	7.22	45.16
Sd	-	0.60	0.68	0.85	0.37	0.41	0.28	0.18	0.87	0.33
ξ1	-	0.57	0.62	0.72	0.36	0.41	0.28	0.17	0.73	0.32
ξ2	-	0.56	0.62	0.72	0.36	0.41	0.27	0.16	0.72	0.31
AUC	836.77	3052.81	3601.59	5111.53	1791.35	2022.37	1487.74	1170.37	5381.03	1627.53
AUC T/R*	-	3.65	4.30	6.11	2.14	2.42	1.78	1.40	6.42	1.94
DP_{30min}	16.24	56.19	66.94	91.46	33.63	38.88	28.23	21.38	96.28	30.55
MDT	15.54	8.74	7.69	7.39	10.38	10.94	11.86	11.27	6.92	11.02
DE	13.95	50.88	60.03	85.19	29.86	33.71	24.80	19.51	89.68	27.12

*AUC T/R- AUC Test/Reference, #FA – Fumaric acid

7.4.2. *In vitro* dissolution studies

The results of the *in vitro* dissolution of the plain drug and their SDs with HPMC and PVP in precipitating medium pH 6.8 phosphate buffer are depicted in Fig 6. $DP_{30\ min}$ values (cumulative percent drug release at 30 min), MDT and DE values for different samples are described in Table 7. From the Table 7 and Fig.6 it was manifested that dissolution rate of pure DPL was very low ($DP_{30\ min}$ 16.24%, MDT of 15.54 min and DE of 13.95%).

SDs with HPMCs exhibited significant enhancement in the dissolution compared to SDs with PVP, plain drug and PMs. PMs with PVP K90 and HPMC E50 also enhanced dissolution rate but effect was not significant as compared to plain drug. Amongst various grades of HPMCs highest improvement in the dissolution was achieved with SDs prepared with HPMC E50 signifying role of intermolecular interactions and steric hindrance in prevention of precipitation of DPL. The solubility results of SDs of HPMC E50 were statistically significantly different ($p<0.05$) as compared with SDs of HPMC E15, HPMC E5, PVP K30 and PVP K90 which was revealed from Bonferroni's multiple comparison test.

From Table 7, it is evident that DP_{30min} and DE values increases while MDT values decreases for all the SD as compared to plain drug. The lowest MDT was showed by SD of HPMC E50, HPMC E15 and HPMC E5 followed by PVP K90 and PVP K30. Similar relationship was observed with DE and DP_{30min} (values increased) and results were in line with MDT values.

Similarity factor f2, Sd and rescingo index ξ1, ξ2 were employed for comparing dissolution profiles of DPL with different samples. The f2 values calculated are presented in Table 7. From the Table 7, it can be concluded that the release profiles of pure DPL and from the samples (SDs with HPMC and PVP) were dissimilar as f2 values below 50 were found for all these comparisons. Similarly, values of similarity factor Sd and rescingo index ξ1, ξ2 were very far away from zero signifying dissimilarity between release profiles of pure drug and samples (SDs with HPMC and PVP). PM with HPMC E50 showed greater improvement in dissolution than PM with PVPK90 which is also reflected from f2, SD, ξ1 and ξ2 values when compared with plain drug. Furthermore, PM with PVPK90 showed marginal improvement in dissolution which was demonstrated by its f2 value (Table 7).

The area under the concentration time (AUC) profile of the dissolution curve was assessed to provide more quantitative information for dissolution results. The results for the AUC and ratio of $AUC_{test}/AUC_{reference}$ are depicted in Table 7. The reference in the each case was crystalline DPL. The results clearly reveal improvement of dissolution by all SDs but HPMC E50 showed clear supremacy over all. It showed 1.42, 1.67, 2.53 and 2.85 fold greater AUC values than HPMC E15, HPMC E5, PVP K90 and PVP K30 respectively.

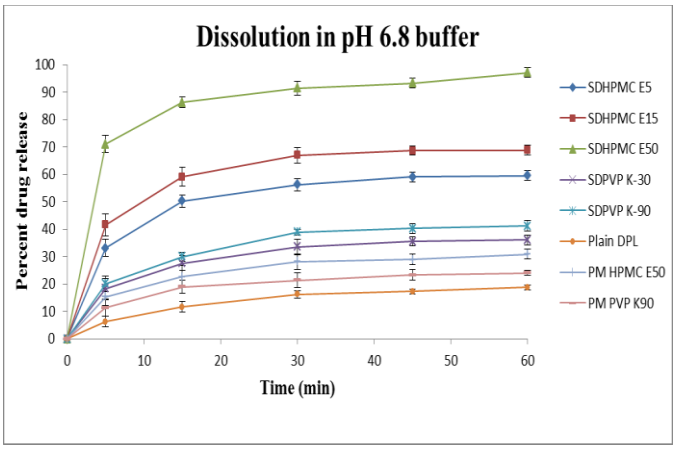

Fig. 6: Cumulative percent drug release of plain DPL, physical mixtures with HPMC E50 and PVP K30, solid dispersions with HPMC E50, HPMC E15, HPMC E5, PVP K90 and PVP K30 in pH 6.8 phosphate buffer.

The results of the *in vitro* dissolution of the plain drug and its complex with fumaric acid in precipitating medium pH 6.8 phosphate buffer is depicted in Fig 7. $DP_{30\ min}$

values (cumulative percent drug release at 30 min), MDT and DE values for sample is described in Table 7.

Complex with fumaric acid exhibited significant enhancement in the dissolution compared to plain drug and PMs. PMs with fumaric acid also enhanced dissolution rate but effect was not significant as compared to complex. From Table 7, it is evident that DP_{30min} and DE values increases while MDT values decreases for the complex with fumaric acid as compared to plain drug.

Similarity factor f2, Sd and rescingo index ξ1, ξ2 were employed for comparing dissolution profiles of DPL with fumaric acid complex. From the Table 7, it can be concluded that the release profiles of pure DPL and from the fumaric acid complex sample were dissimilar as f2 values below 50 were found for all these comparisons. Similarly, values of similarity factor Sd and rescingo index ξ1, ξ2 were very far away from zero signifying dissimilarity between release profiles of pure drug and fumaric acid complex sample.

The area under the concentration time (AUC) profile of the dissolution curve was assessed to provide more quantitative information for dissolution results. The results for the AUC and ratio of $AUC_{test}/AUC_{reference}$ are depicted in Table 7. The reference was crystalline DPL. The results clearly reveal improvement of dissolution by complex formation with fumaric acid.

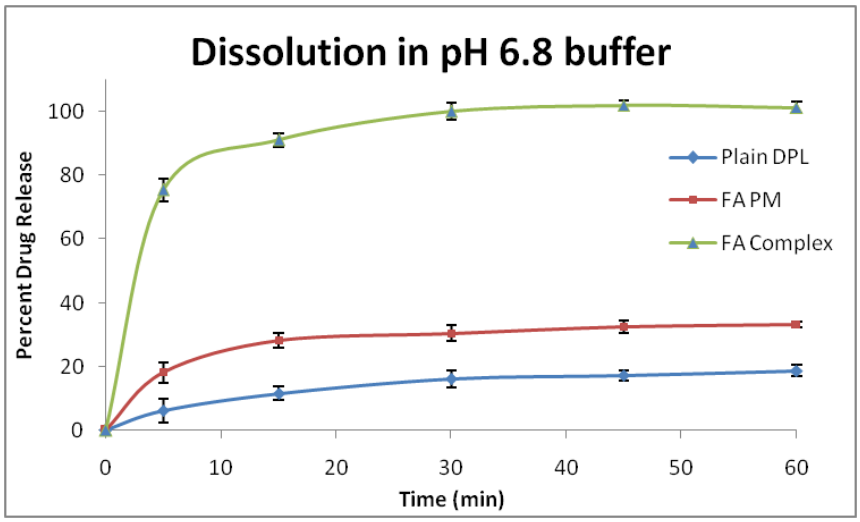

Fig. 7: Cumulative percent drug release of plain DPL, physical mixtures with fumaric acid and complex with fumaric acid in pH 6.8 phosphate buffer.

7.4.3. Supersaturated dissolution testing

The pH change over dissolution i.e. following acid to neutral pH transition explicitly signifies the importance of physical and chemical properties of diverse polymers on maintaining and stabilizing supersaturation. Thus following 2 h of dissolution in acidic medium, additional 4 h dissolution was carried out in phosphate buffer pH 6.8 to study extent of supersaturation stabilization and precipitation of DPL upon pH transition. At the end of 2 h in acidic medium, the extent of supersaturation was similar for HPMC and PVP grades. Upon pH transition from acidic to neutral, it was observed that maximum stabilization was provided by HPMC and amongst its different grades HPMC E50 provided substantial stabilization followed by HPMC E15 and HPMC E5. On the contrary, two molecular weight grades of PVP provided moderate inhibition to stabilization. The HPMC E50 based formulation showed minimal precipitation with approximately 78% drug remaining in solution upto 4 h after pH transition. The HPMC E15 and HPMC E5 formulation showed approximately 53 % and 42% DPL remaining in the solution at the end of 4 h after pH transition. On the contrary, significant precipitation was observed with both grades of PVP demonstrating approximately 28% for PVP K90 and 25% for PVP K30 remaining drug in solution at the end of 3 h after pH transition. Thus, the order of the polymers for inhibiting precipitation and maintaining supersaturation after pH transition was HPMC E 50 > HPMC E 15 > HPMC E5 > PVP K90, PVP K30. Similar results were obtained by Williams III et. al. where they found HPMC was superior than PVP for inhibiting precipitation of itraconazole [28].

The disparity observed between various polymeric stabilizers reveal involvement of physical and chemical aspects of polymeric stabilizer that affect rate of precipitation upon pH transition. As observed, irrespective of polymer grades, HPMC was found superior in comparison to PVP. This signifies role of molecular interaction between drug and polymer. PVP acts as proton acceptor due to carbonyl groups present in its backbone whereas HPMC acts as proton donor due to numerous free hydroxyl group present its backbone. Here strong interaction (hydrogen bonding) was observed between HPMC and DPL and no interaction between PVP and DPL. The same can be inferred from FT-IR studies. It is due to this hydrogen bonding between HPMC and DPL it is more beneficial in inhibiting precipitation than PVP.

Secondly, in case of HPMC, effect of molecular weight on providing stabilization to supersaturation was prominently seen in comparison to PVP where only modest effect was observed between different viscosity grades. It is anticipated that higher molecular weight grades will increase the viscosity of the solution due to increase chain entanglements and will provide greater steric hindrance to nucleation and crystal growth of DPL. The increase in viscosity of solution hinders the drug diffusion into the bulk of the solution and thus more of the drug will remain in intimate contact with the stabilizing polymer. Here it was observed that effect of molecular weight was prominently seen in HPMC resulting in greater stabilization provided by HPMC E50 followed by HPMC E15 and then HPMC E5 which may be due to strong interactions observed between DPL and HPMC. As no intermolecular interactions have been observed between PVP grades, the effect of molecular weight was less pronounced. Thus, besides reducing diffusivity of DPL in bulk solution by increasing viscosity, strong intermolecular interactions played a critical role in providing substantial stabilization to precipitation of DPL.

The area under the concentration time (AUC) profile of the dissolution curve was assessed to provide more quantitative information for dissolution results. The AUC provides estimation of both degree and duration of supersaturation thus portraying a complete picture of the extent of supersaturation. The results clearly stipulate the dominance of SDHPMC E50 in respect to maintaining DPL supersaturation and inhibiting precipitation. The HPMC E50 demonstrated 16.4%, 23.79%, 40.52% and 44.91% greater mean AUC values than HPMC E15, HPMC E5, PVP K-30 and PVP K-90 respectively.

In case of pH modifier, supersaturated dissolution was carried out in the similar manner as discussed above. At the end of 2 hr in acidic medium, it showed similar extent of supersaturation as in case of HPMC and PVP. Upon transition from the acid to neutral pH transition, substantial stabilization was provided by drug fumaric acid complex and showed minimal precipitation with approximately 81% drug remaining in solution after pH transition. Hence, pH modifier also provided similar effect to HPMC E50 on inhibiting drug precipitation upon acid to neutral pH transition.

7.4.4. Characterization of solid dispersion

7.4.4.1. Differential scanning calorimetry (DSC) study

DSC study facilitates recognition of all processes in which energy is required or produced (i.e., endothermic or exothermic phase transformations). The thermal behavior of the DPL, its PM with HPMC E50 and PVP K90 and prepared SDs with different molecular weight grades of HPMC and PVP was studied by DSC. The DSC thermograms for pure DPL, PM with PVP K90 and HPMC E50 and SDs with HPMC E5, HPMC E15, HPMC E50, PVP K30 and PVP K90 are shown in Fig. 8. DSC thermogram of pure DPL showed sharp melting endotherm at about 165◦C revealing form-II of DPL. The DSC thermogram of pure PVP K90 and HPMC E50 were taken on behalf of all its respective molecular weight grades. The DSC thermogram of PVP K90 showed a broad endotherm ranging from 60 to 110 °C due to the presence of residual moisture in PVP while HPMC E50 also showed similar broad endotherm due to residual moisture. Both PVP and HPMC showed absence of any peak besides that of residual water revealing its amorphous nature. PM were prepared with the highest grade of each polymer PVP and HPMC. PM with PVP K 90 showed melting peak of the drug at around165◦C and broad endotherm between 60◦C to 110◦C due to residual moisture in PVP. PM with HPMC E50 also showed similar behavior. SD with both grades of PVP and all three grades of HPMC at 50%w/w showed complete absence of drug peak at 165 °C. This complete absence of the DPL peak reveals that DPL was amorphous inside the HPMC and PVP matrix. Thus, SD was completely formed for both polymers and also with all of its molecular grades. The reduction in crystallinity and improved wettability of DPL in the SD can also be seen in the PXRD data and MDT values (Table 7) respectively.

DSC thermograms of plain drug, fumaric acid, PM with fumaric acid and complex formation with fumaric acid is shown in Fig. 9. DSC thermograms of complex revealed some other peaks in addition to drug peak indicating it interaction with drug and causing possible changes in drug crystal or new bond formations.

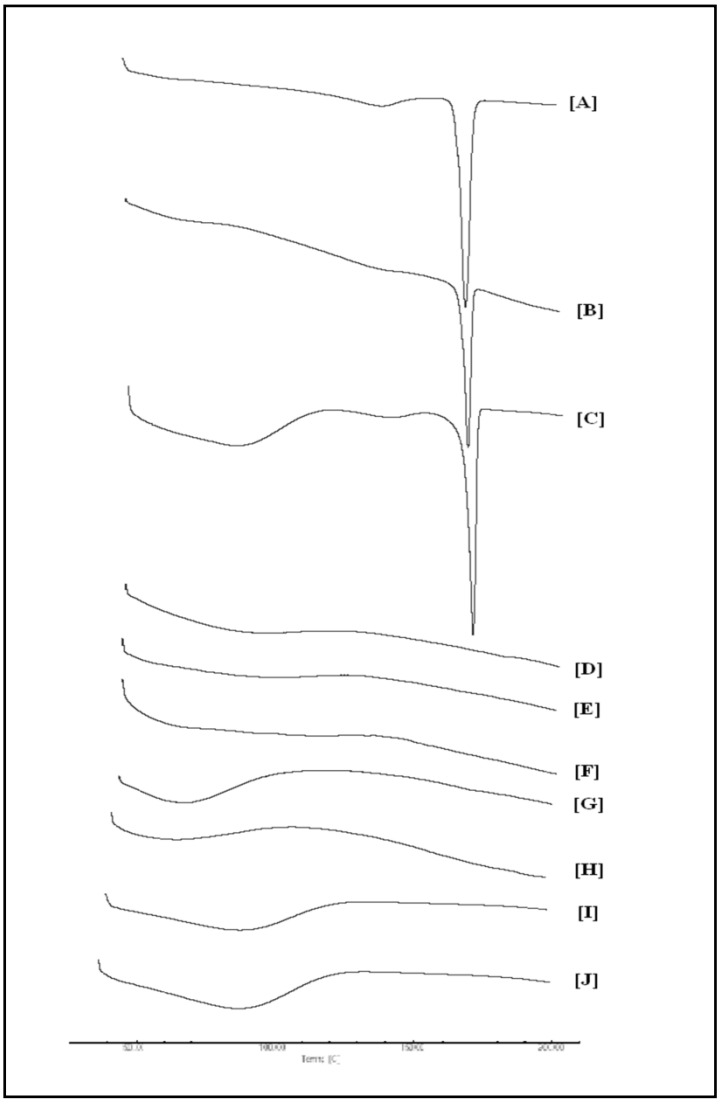

Fig. 8: DSC spectra of [A] Plain drug, [B] PM HPMC E50, [C] PM PVP K-90, [D] SD HPMC E 50, [E] SD HPMC E 15, [F] SD HPMC E 5, [G] SD PVP K30, [H] SD PVP K90, [I] HPMC E50 and [J] PVP K90.

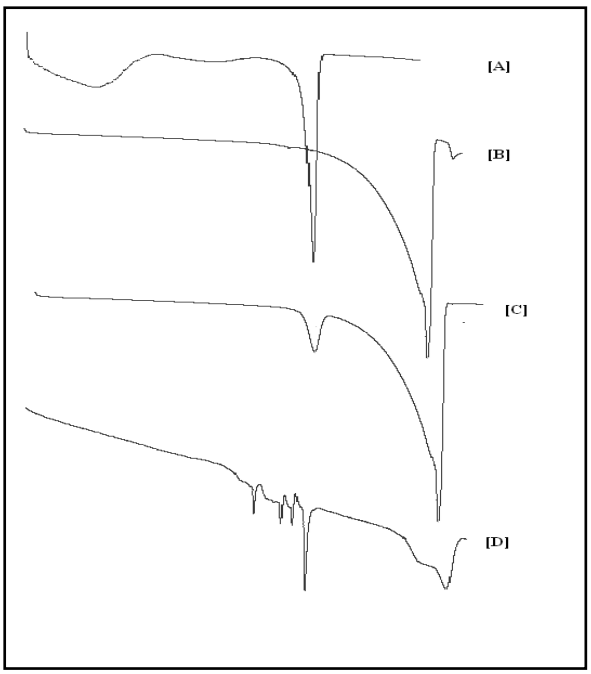

Fig. 9: DSC spectra of [A] Plain drug, [B] Fumaric acid, [C] PM Fumaric acid, [D] Fumaric acid complex

7.4.4.2. Powder X-Ray Diffraction Study

The PXRD spectra of pure DPL, PVP K90, HPMC E50, PMs with PVP K90 and HPMC E50 and SDs with HPMC E5, HPMC E15, HPMC E50, PVP K30 and PVP K90 are shown in Fig. 10. The PXRD spectra of DPL revealed characteristic peaks of 2θ at 7.9881, 10.1827, 13.3151, 17.3282, 18.7113, 20.7806, 22.5315 and 30.2972. The numerous distinct peaks indicated that DPL was present in crystalline form. PVP K90 and HPMC E50 indicated the halo pattern revealing amorphous nature of polymers. The PM with PVP and HPMC revealed characteristic peaks of the DPL at the same position as that of pure drug indicating presence of free drug. The SDs with different grades of both the polymers PVP and HPMC showed halo pattern and complete absence of major diffraction peaks of DPL signifying DPL was present in amorphous form inside PVP and HPMC matrix. Thus, successful SD was formed with both the polymers. Thus the enhanced solubility and dissolution from the SDs was due to the amorphous nature. This was also supported by the MDT values of SDs as shown in Table 7.

The PXRD of pure DPL, fumaric acid, PM fumaric acid and complex with fumaric acid is depicted in Fig. 11. The complex with fumaric acid showed that some of the

characteristic peaks of DPL were modified or were absent. Thus the results were in line with DSC data indicating that the complex created change in the crystal habit of the drug and modified it.

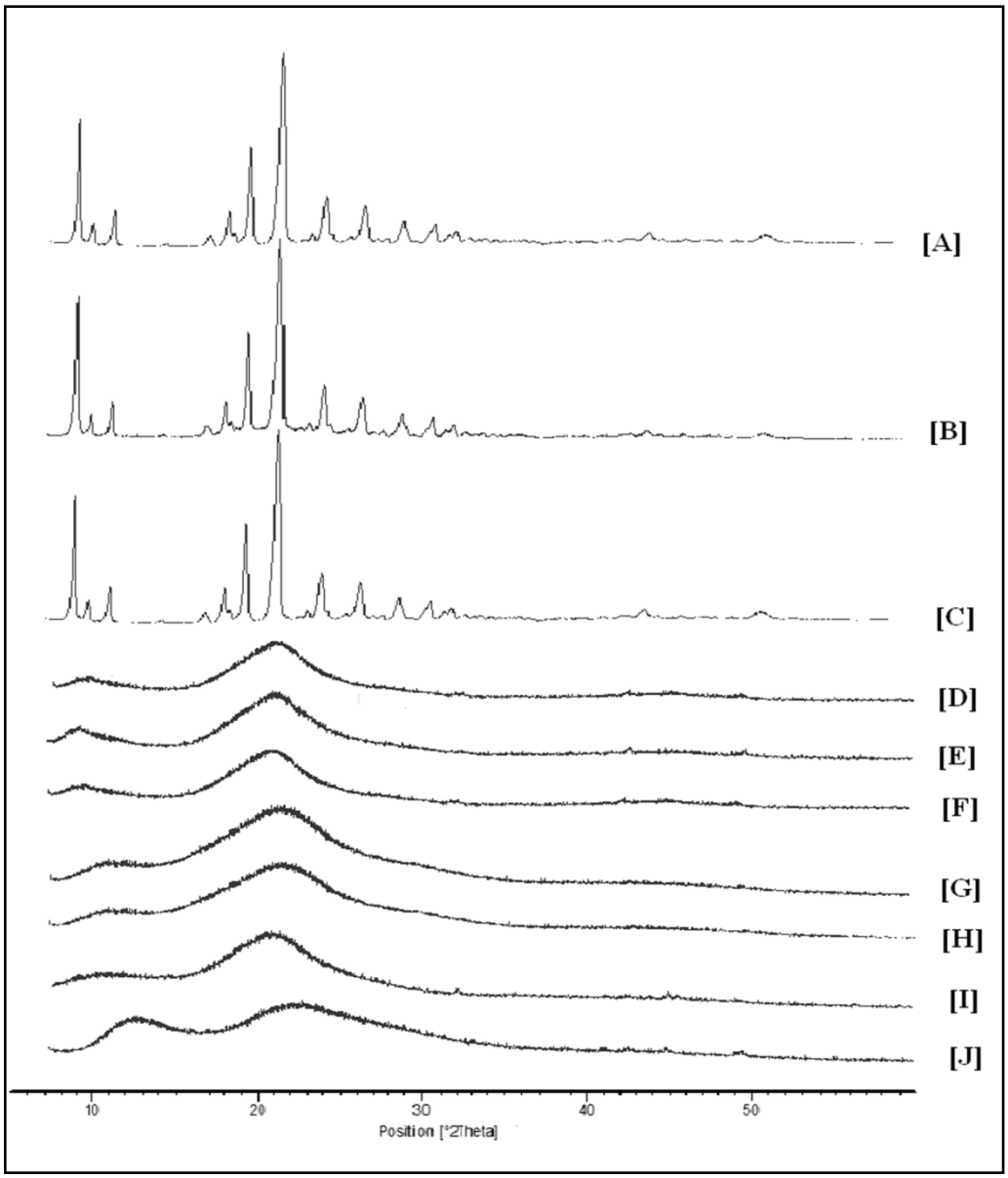

Fig. 10: PXRD spectra of [A] Plain drug, [B] PM HPMC E50, [C] PM PVP K-90, [D] SD HPMC E 50, [E] SD HPMC E 15, [F] SD HPMC E 5, [G] SD PVP K30, [H] SD PVP K90, [I] HPMC E50 and [J] PVP K90.

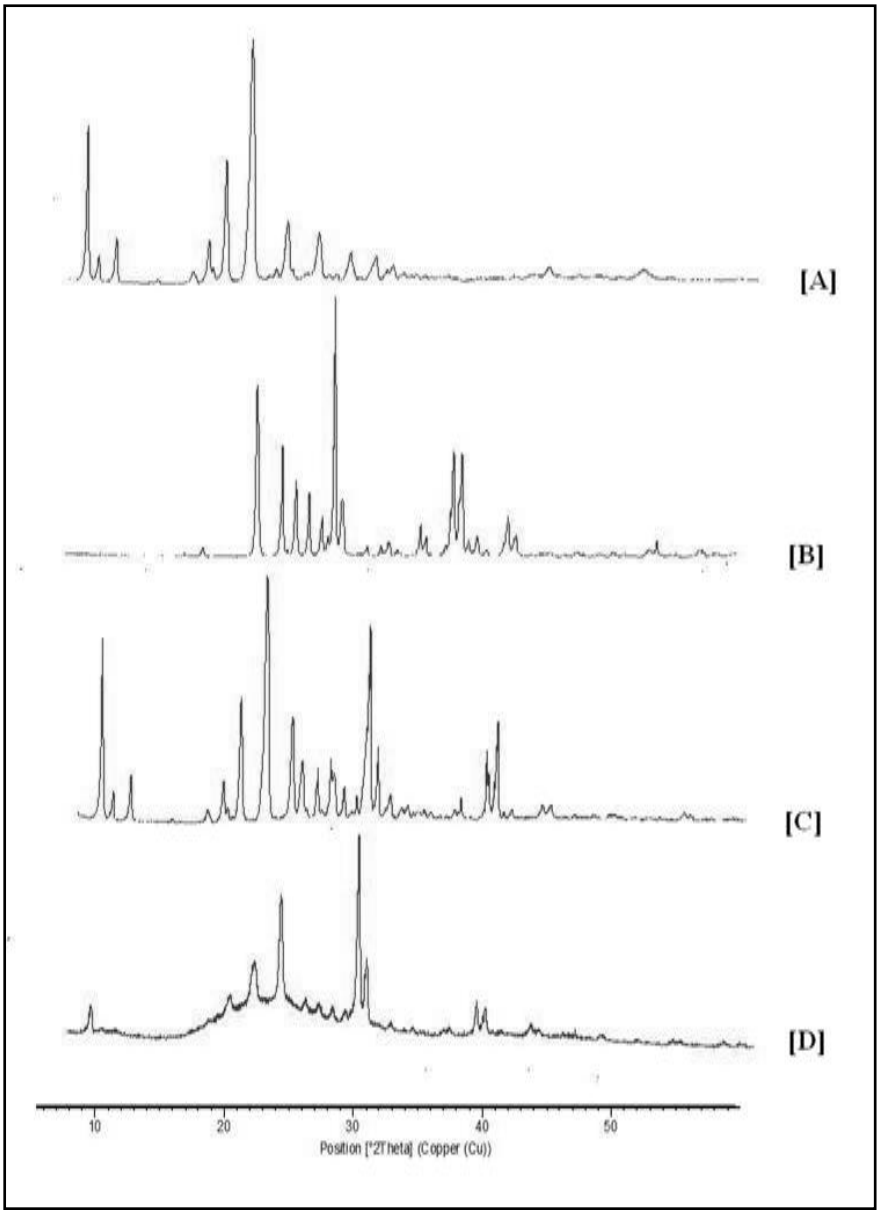

Fig. 11: PXRD spectra of [A] Plain drug, [B] fumaric acid, [C] PM fumaric acid, [D] Complex with fumaric acid

7.4.4.3. Fourier transform infra-red (FT-IR) spectroscopy study

The FT-IR spectra of pure DPL, PVP K90, HPMC E50, PMs with PVP K90 and HPMC E50 and SDS with HPMC E5, HPMC E15, HPMC E50, PVP K30 and PVP K90 are shown in Fig. 12. The FT-IR spectra of DPL revealed characteristic peaks at 1535 cm^{-1} and 1360 cm^{-1} peaks corresponding to C=N ring and C-N bonds, 2930 cm^{-1} and 2852cm^{-1} corresponding to asymmetrical and symmetrical stretch of CH_2 group and 3377 cm^{-1} and 3303 cm^{-1} corresponding to OH stretching vibration. PVP K-90

showed important bands at 2925 cm^{-1} (C–H stretch) and 1652 cm^{-1} (C=O). A very broad band was also visible at 3300 cm−1, which was due to the presence of water verifying the broad endotherm detected in the DSC experiments while HPMC showed important bands at 3050–3750 cm^{-1} and are attributed to the –O–H stretching and the triple peak in the so-called finger print spectrum area of C–O– is at 960–1230 cm^{-1}. The spectra of PMPVP 50%w/w and PMHPMC 50% w/w can be simply regarded as the superposition of those of DPL and PVP or HPMC. No difference was seen in the position of the absorption bands of DPL and HPMC or PVP. In case of SDs contrasting observations was found. In case of SDs with PVP showed no change in spectra as that from plain drug and PM suggesting no chemical interaction between DPL and PVP and subsequently no hydrogen bond formation. On the contrary, interactions was observed between HPMC and drug characterized by changing in C-N band at 1360 cm^{-1} and C=N band at 1535 cm^{-1}. Thus it could be anticipated that OH group of the polymers might be interacting with C-N group present in DPL through hydrogen bonding. Thus strong intermolecular interactions were observed between HPMC but not for PVP.

The FT-IR of pure DPL, fumaric acid, PM fumaric acid and complex with fumaric acid is depicted in Fig. 13. The complex with fumaric acid showed that some of the characteristic peaks of DPL were modified. Thus the results were in line with DSC data indicating that the complex created change in the crystal habit of the drug and might have modified it.

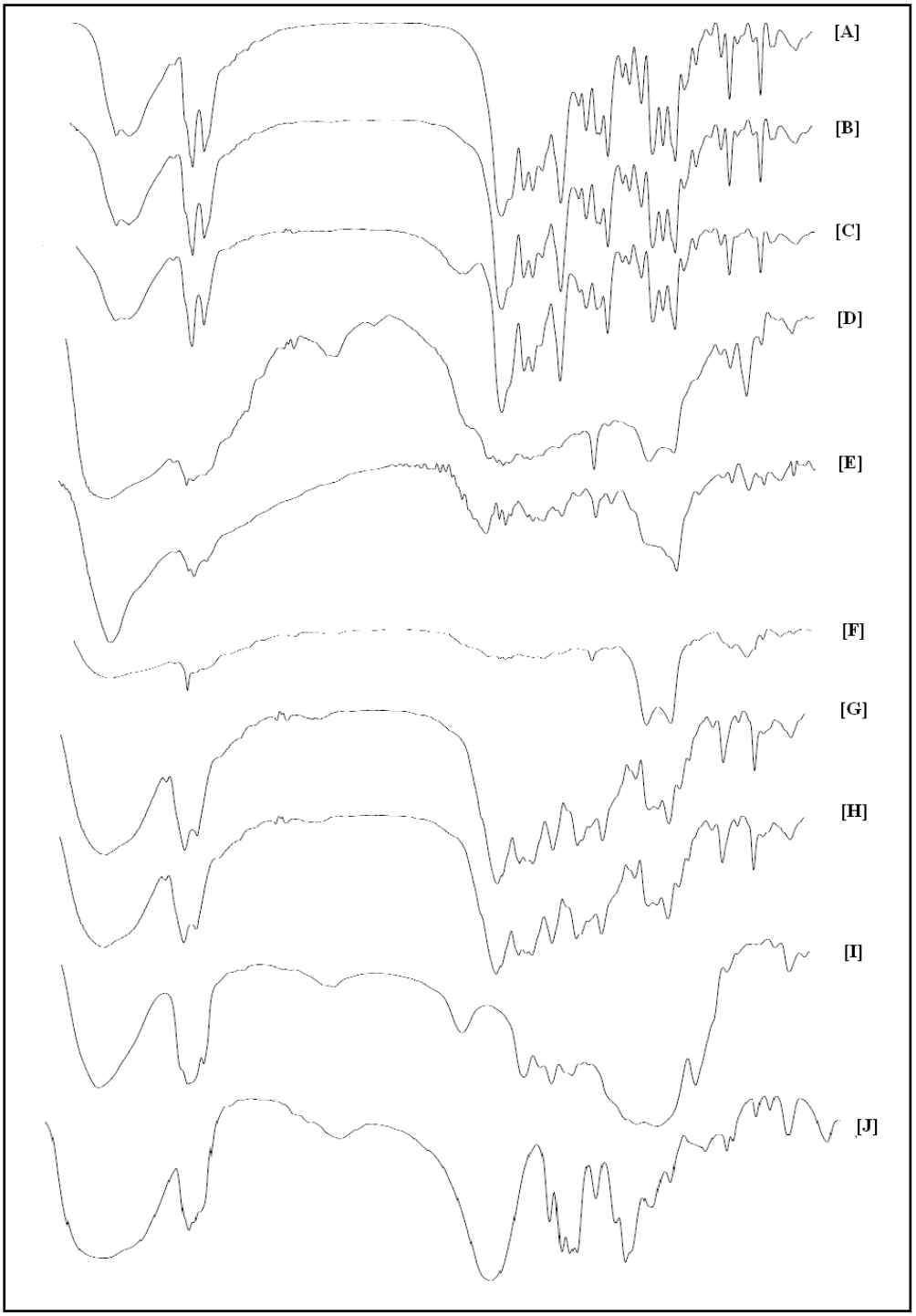

Fig. 12: FT-IR spectra of [A] Plain drug, [B] PM HPMC E50, [C] PM PVP K-90, [D] SD HPMC E 50, [E] SD HPMC E 15, [F] SD HPMC E 5, [G] SD PVP K30, [H] SD PVP K90, [I] HPMC E50 and [J] PVP K90.

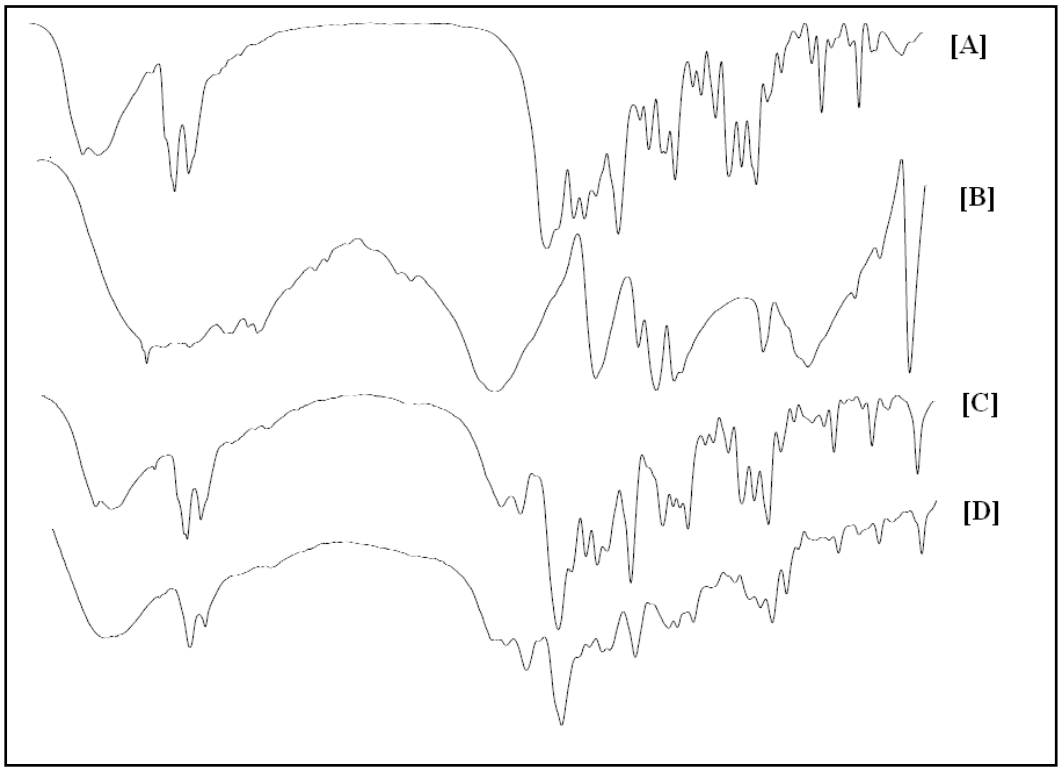

Fig. 13: FT-IR spectra of [A] Plain drug, [B] fumaric acid, [C] PM fumaric acid, [D] SD fumaric acid

7.4.5. Formulation studies

The formulation studies were carried out with optimized formulation SD HPMC E50 (50%w/w) and complex formation with fumaric acid (30%w/w). DSC study revealed no drug interaction with the chosen excipients.

7.4.5.1. Flow properties of powder blend

Evaluating powder flow properties is very crucial for direct compression as it is well known that poor powder flow may cause several intricacies during compression. The flow properties of final blend containing SDs of DPL with HPMC E50 and complex with fumaric acid were assessed using Carr's index, Hausner's ratio and angle of repose. The powder blend of SD HPMC E50 showed Carr's index, Hausner's ratio and angle of repose of 17.64, 1.21 and 32.6 respectively and that of complex with fumaric acid 19.10, 1.22 and 33.9 respectively indicating fair flow properties and making it suitable for tabletting.

7.4.5.2. Characterization of tablet

Rapid disintegrating tablets were prepared for optimized composition of SD with HPMC E50 and complex formation with fumaric acid. The prepared tablets were studied for their physical properties like weight variation, hardness, friability, disintegration time and drug content. The results of formulation revealed that the tablets comply with the standards. The weight variation of all the tablets was uniform as indicated from low SD values (SD < 3%). Hardness of tablets was found to be between 3.5 to 4.5 indicating satisfactory crushing strength. The friability was found to be below 0.5 % indicating good mechanical resistance of the tablet and ability to withstand during packaging and shipment. The drug content of formulations was found between 98.4 to 101.6% with low standard deviation, revealing satisfactory results for drug content of the prepared batches. The disintegration time for both the formulation was found to be less than 120 sec.

The release profiles of the conventional tablets containing plain DPL and tablets containing SD HPMC E50 and complex with fumaric acid in pH 6.8 phosphate buffer are depicted in Fig.14. It can be clearly observed from the Fig. 14 higher dissolution of tablets containing SD and complex than plain DPL tablets. The same can be inferred form MDT value, DP_{30min} and DE as shown in Table 8. The MDT value of the pure DPL tablets was very high which decreased to a greater extent for tablets containing SD with HPMC E50 and complex with fumaric acid. Moreover DP_{30min} and DE were also higher for SD HPMC E50 and complex with fumaric acid tablets as compared with those of conventional tablets.

The release profile comparisons between different DPL formulations were made by similarity factor f2, similarity factor Sd and rescingo index $\xi 1$ and $\xi 2$. The calculated values of the various indices are depicted in Table 8. From the Table 8, it is obvious that release profile from the samples (SD HPMC E50) and pure DPL was dissimilar since f2 values for all the comparisons were less than 50, similarity factor Sd and rescingo index $\xi 1$ and $\xi 2$ were far away from zero. Similar results were obtained for tablets containing fumaric acid complex (Table 8) Thus, tablet formulation containing SD HPMCE50 and fumaric acid complex were obviously superior to conventional tablets containing DPL due to improve solubility and better dissolution characteristics.

Moreover, supersaturated dissolution testing results of tablets prepared with HPMC E50 revealed similar results with that of solid dispersion of SDHPMC E50. The tablets (SD HPMC E50) attained similar supersaturation upon pH transition to neutral media (~76%) which was similar to that of solid dispersion (~78%). Thus, SD can be efficiently formulated into tablets for improving dissolution characteristics and stabilization of supersaturation.

Similar results were obtained for supersaturated dissolution testing of tablets containing fumaric acid complex. The tablets containing fumaric acid complex attained similar supersasturation upon pH transition to neutral media (~78%) which was similar to that of solid dispersion (~81%). Thus, fumaric acid complex tablets can be efficiently formulated into tablets for improving dissolution characteristics and stabilization of supersaturation.

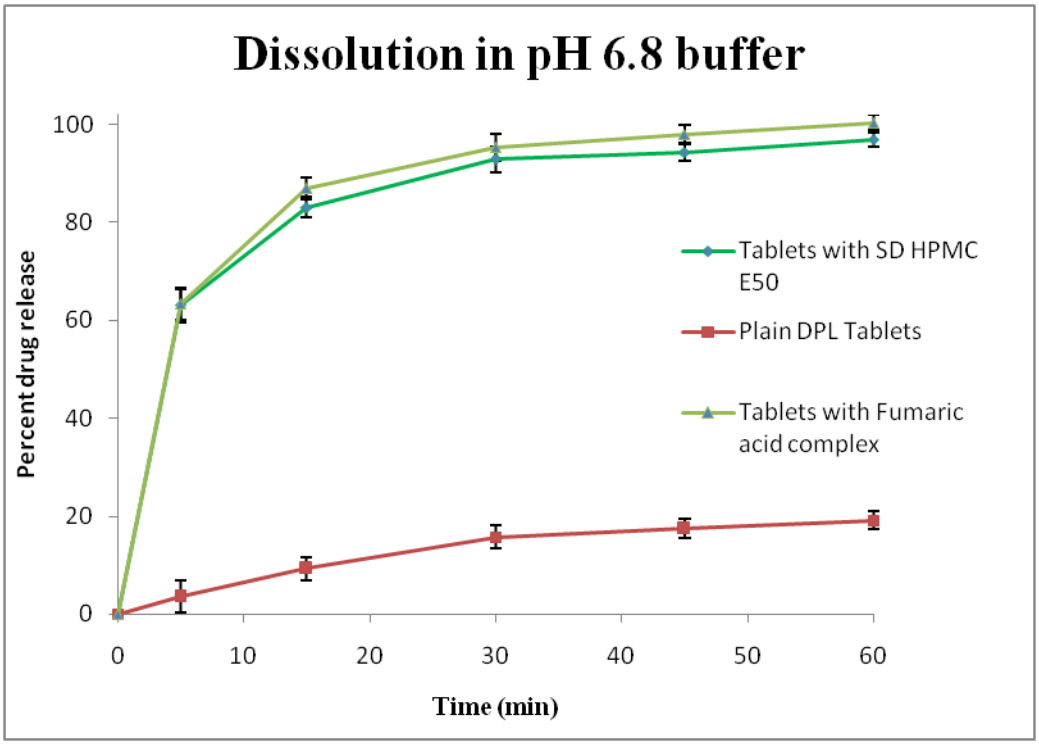

Fig. 14: Cumulative percent drug release of plain DPL tablets, tablets with SD HPMC E50 and tablets with fumaric acid complex in pH 6.8 phosphate buffer.

Table 8: Table representing solubility ratio, various indices for comparison of dissolution profiles, cumulative percent drug released at 30 min (DP_{30min}), Mean Dissolution Time (MDT) and Dissolution Efficiency (DE) for tablets containing plain drug, solid dispersion with HPMC E50 and fumaric acid complex.

	Crystalline DPL tablets	SDHPMC E50 tablets	Fumaric acid complex tablets
f2	-	8.70	7.85
Sd	-	0.93	0.93
ξ1	-	0.73	0.74
ξ2	-	0.73	0.73
AUC	780.93	5045.55	5216.03
AUC T/R*	-	6.46	6.68
DP_{30min}	15.69	92.85	95.28
MDT	19.11	7.94	8.04
DE	13.02	84.09	86.93

7.4.6. *In vitro* cell line studies

Fig. 15 gives pictorial representation of containing Caco-2 cells with culture media.

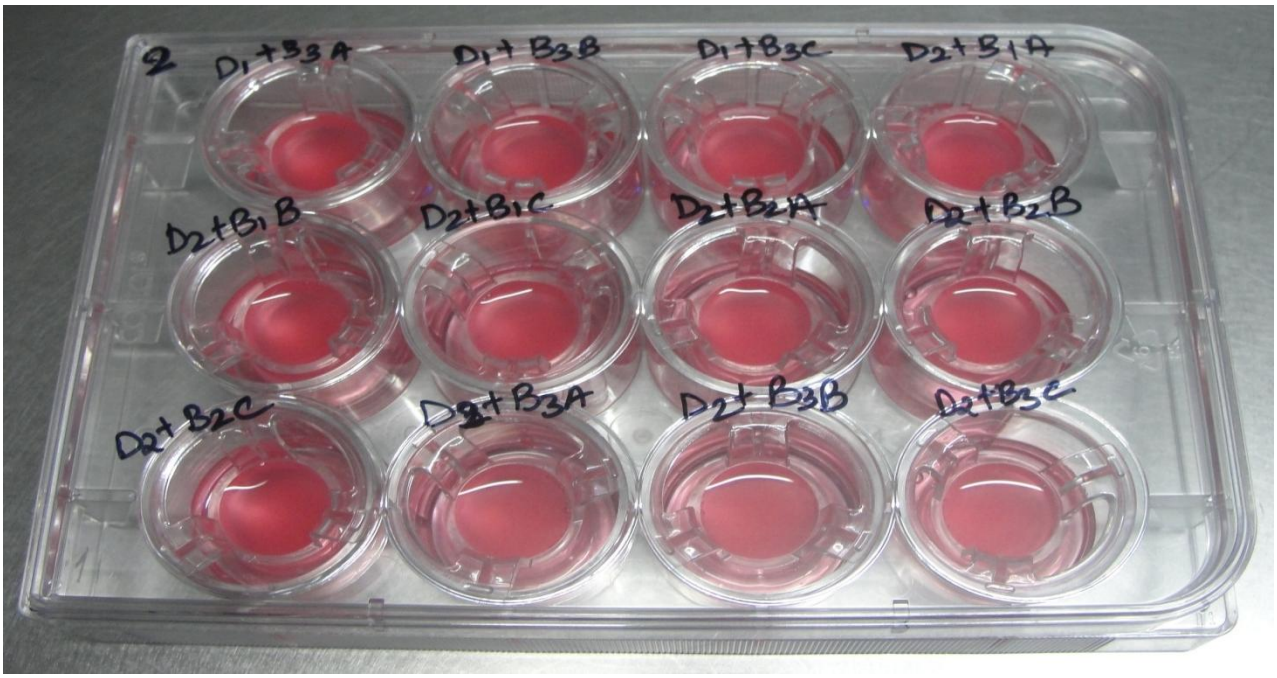

Fig. 15: The diagram of Transwell (12 wells, 1.13 cm^2 polyester, 0.4 µm pore size) containing Caco-2 cells with culture media.

7.4.6.1. Cell monolayer integrity

The TEER value measurement is an indicator of epithelial tight junction integrity and measures the resistance of cell monolayer. The cell monolayer exhibited a resistance of 460 – 490 ohms prior to transport experiment. The TEER values did not significantly changed after completion of experiment for the formulations studied as shown in Fig. 16 indicating no disruption or opening of epithelial tight junction for increasing permeability of drug.

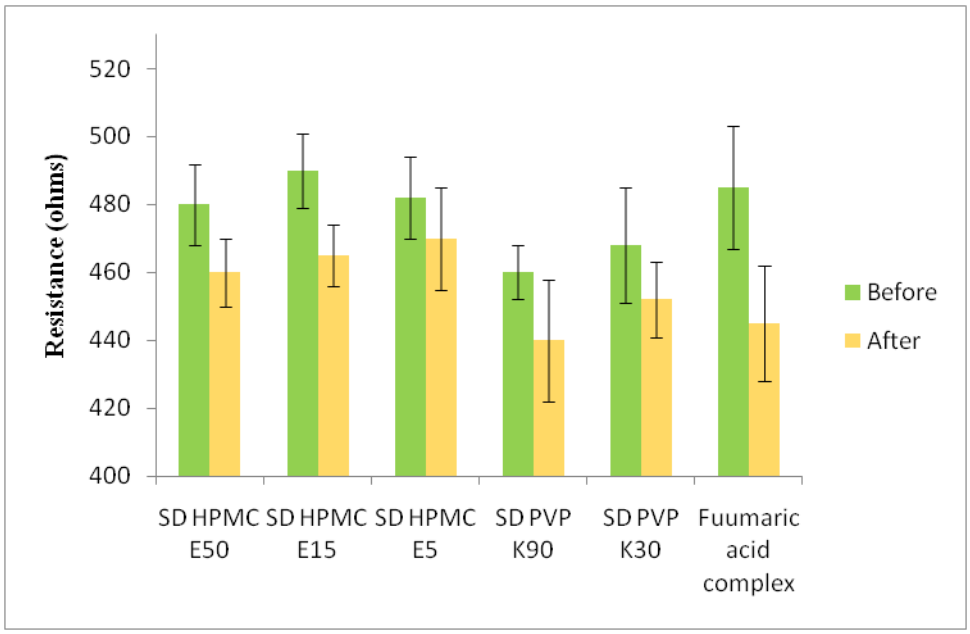

Fig. 16: Effect of various formulations on cell monolayer integrity. TEER values ± SD (n = 4) for wells before and after exposure to 4 h.

7.4.6.2. Transport experiments

The permeability experiments for unformulated DPL and DPL SDs with HPMC and PVP and DPL complex with fumaric acid were carried out to assess the contribution of type of formulation on increasing permeability of DPL. DPL alone per se showed a P app value of $2.26 \pm 1.51 \times 10^{-6}$ cm/s . In comparison to plain DPL, DPL SDs with HPMC and PVP as well as DPL complex with fumaric acid exhibited enhanced P app values as shown in Table 9. Maximum enhancement of about 6.73 times and 6.99 times was shown by DPL SD with HPMC E 50 and DPL complex with fumaric acid respectively.

Table 9: P app values (Mean ± SD) of different samples (n = 4) and the increment in P app value as compared to unformulated DPL.

Name	P app × 10^{-6} cm/s (Mean ± SD)	Enhancement ratio in P app
Unformulated DPL	2.26± 1.51	-
HPMC E50 SD	15.21±1.39	6.73
HPMC E15 SD	10.85±1.33	4.80
HPMC E 5 SD	7.45±1.28	3.30
PVP K90 SD	6.11±1.09	2.70
PVP K30 SD	5.15±1.15	2.54
Fumaric acid complex	6.53±1.55	6.99

7.4.6.3. Assessment of cell viability or MTT assay

During the MTT assay, damaged or dead cells show reduced or no catalytic activity. As the duration for permeability experiments was 4 h, MTT assay was also performed for exposure time of 4 h. As shown in Fig. 17, neither the formulation nor individual excipients showed significant cell death or cytotoxicity as compared to the control group. DPL formulations and all the excipients tested showed cell viability > 90% revealing no cytotoxic effect of formulation and excipients on cell monolayer during the 4 h incubation period.

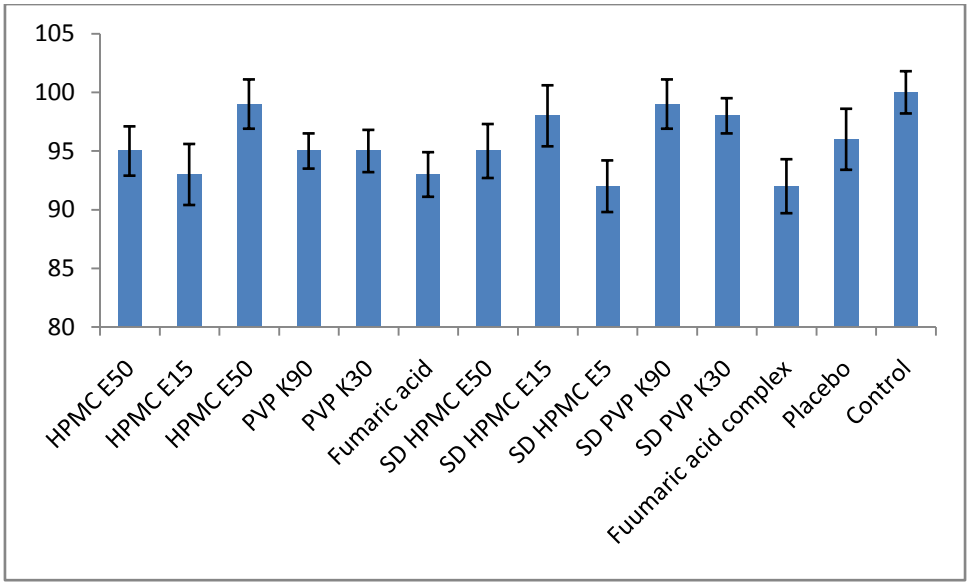

Fig. 17: Cytotoxicity studies showing the % cell viability of Caco-2 cells after exposure to different samples for 4 h (n = 6).

7.4.7. Stability studies

The optimized formulation of SD HPMC E50 and complex with fumaric acid showed insignificant change under the conditions of storage for parameters like appearance, drug content and *in vitro* drug release. The similarity factor (f2) [18] was employed for comparison of dissolution profiles on each time point. It ranged from 78 to 85. Therefore comparable *in vitro* dissolution as of initial samples was observed.

Conclusion

The SDs of DPL were prepared with different molecular weight grades of HPMC and PVP. The solubility studies revealed increase in solubility with both the polymers. The DSC and PXRD study revealed that the drug was present as amorphous form inside polymeric matrix of PVP or HPMC. The acid to neutral pH transition dissolution study revealed the importance of intermolecular interactions between DPL and polymers. The HPMC E50 was found out to be the best polymer for inhibiting precipitation and extending the supersaturation. The effect of molecular weight was prominently seen in case of HPMC but not in case of PVP which may be due to interaction between drug and polymer which was confirmed from FT-IR studies. Finally, the rapid disintegrating tablets were prepared with HPMC E50 and results revealed significant improvement in dissolution as compared to conventional DPL tablet which was clearly evident from MDT, DP_{30min} and DE values of prepared formulations.

Preparation of complex with fumaric acid also increased solubility and prevented precipitation and extended supersaturation upon acid to neutral pH transition similar to that of HPMC E50. Rapid disintegrating tablets prepared with fumaric acid also resulted in significant improvement in dissolution as compared to conventional DPL tablet.

In nutshell, judicious selection of polymer is needed for preparing SD/complex which can stabilize and maintain supersaturation of DPL for longer period of time. The formulations develop with HPMC E50 and fumaric acid can be a promising alternative method for attaining greater supersaturation upon acid to neutral pH transition.

7.6. References

1. Xu, L., Luo, Y., Feng, J., Xu, M., Tao X., He H., Tang X., 2012. Preparation and in vitro–in vivo evaluation of none gastric resident dipyridamole (DIP) sustained-release pellets with enhanced bioavailability. Int. J. Pharm. 422, 9-16.
2. Terhaag, B., Donath, F., Le Petit, G., Feller, K., 1986. The absolute and relative bioavailability of dipyridamole from different preparations and the in vitro-in vivo comparison. Int. J. Clin. Pharmacol. Ther. Toxicol. 24, 298-302.
3. Kim, H.H., Liao, J.K., 2008. Translational therapeutics of dipyridamole. Arterios. Thromb. Vascul. Biol. 28, 39–42.
4. Clarke's Isolation and Identification of Drugs, 1986. 2nd ed., A.C. Moffat, Ed., The Pharmaceutical Press, London, pp. 562.
5. The Merck Index, 1996. 12th edn., S. Budavari, ed., Merck and Co., NJ, pp. 567.
6. Khalil, A., Belal, F., Al-Badr, A.A., 1976. Dipyridamole. In: Florey, K. (Ed.), Analytical Profiles of Drug Substances. Academic Press, New York, 31, pp. 215–278.
7. Dipyridamole - Pubchem. Available at http://pubchem.ncbi.nlm.nih.gov/ compound /dipyridamole#section=Top
8. Dipyridamole - Dailymed. Available at http://dailymed.nlm.nih.gov/dailymed/ drugInfo.cfm?setid=dcf785b2-e923-43bf-93bb-00a9501479f4.
9. FitzGerald, G.A., 1987. Dipyridamole. N. Engl. J. Med., 316, 1247.
10. Harker, L.A., Kadatz, R.A., 1983. Mechanism of action of dipyridamole. Thromb Res. Suppl. 4, 39-46.
11. ICH harmonised tripartite guideline, November 2005. Validation of analytical procedures: text and methodology. Q2 (R1).
12. Yamashita, K., Nakate, T., Okimoto, K., Ohike, A., Tokunaga, Y., Ibuki, R., Higaki, K., Kimura, T., 2003. Establishment of new preparation method for solid dispersion formulation of tacrolimus. Int J Pharm. 267:79–91.
13. Gao, P., Guyton, M.E., Huang, T., Bauer, J.M., Stefanski, K.J., Lu, Q., 2004. Enhanced oral bioavailability of a poorly water soluble drug PNU-91325 by supersaturatable formulations. Drug Dev Ind Pharm. 30: 221–229.
14. Okimoto, K., Miyake, M., Ibuki, R., Yasumura, M., Ohnishi, N., Nakai T., 1997. Dissolution mechanism and rate of solid dispersion particles of nilvadipine with hydroxypropylmethylcellulose. Int J Pharm. 159:85–93.

15. Suzuki, H., Sunada, H., 1998. Influence of water-soluble polymers on the dissolution of nifedipine solid dispersions with combined carriers. Chem Pharm Bull. 46: 482–487.
16. Yokoi, Y., Yonemochi, E., Terada, K., 2005. Effects of sugar ester and hydroxypropyl methylcellulose on the physicochemical stability of amorphous cefditoren pivoxil in aqueous suspension. Int J Pharm. 290: 91–99.
17. Pharmacopeia US. National Formulary. USP 30-NF 25. Rockville, MD: USP; 2006.
18. Moore, J.W., Flanner, H., 1996. Mathematical comparison of dissolution profiles. Pharm Technol. 20: 64–74.
19. Gohel, M.C., Panchal, M.K., 2000. Comparison of in vitro dissolution profiles using a novel, model-independent approach. Pharm Technol. 24: 92-102.
20. Gohel, M.C., Panchal, M.K., 2002. Novel use of similarity factor f2 and Sd for the development of diltiazem HCl modified-release tablets using a 3^2 factorial design. Drug Dev Ind Pharm. 28:77-87.
21. Rescigno, A., 1992. Bioequivalence. Pharm Res. 9:925–928.
22. Costa, P., Lobo, J.M.S., 2001. Modeling and comparison of dissolution profiles. Euro J Pharm Sci. 13:123–133.
23. Reppas, C. Nicolaides E. Analysis of drug dissolution data. In Oral drug absorption prediction and assessment; Dressman, J. B., Lennernäs, H., New York: Marcel Dekker; 2000. p. 229–254.
24. Khan, K.A., 1975. The concept of dissolution efficiency. J Pharm Pharmacol. 27:48–49.
25. Khan, K.A., Rhodes, C.T., 1972. Effect of compaction pressure on the dissolution efficiency of some direct compression systems. Pharm Act Helv. 47: 594–607.
26. Wahlang, B., Pawar YB, Bansal AK., 2011. Identification of permeability-related hurdles in oral delivery of curcumin using the Caco-2 cell model. Eur J Pharm Biopharm. 77(2):275-82.
27. ICH harmonised tripartite guideline, February 2003. Stability testing of new drug substances and products Q1A(R2).
28. Miller, D.A., DiNunzio, J.C., Yang, W., McGinity, J.W., Williams, III RO., 2008. Enhanced in vivo absorption of itraconazole via stabilization of

supersaturation following acidic-to-neutral pH transition Drug Dev Ind Pharm. 34:890–902.